Geophys. J. Int. (1998) **135,** 362–374

Palaeomagnetism of the continental sector of the Cameroon Volcanic Line, West Africa

R. U. Ubangoh[1], I. G. Pacca[1] and J. B. Nyobe[2]

[1] *Instituto Astronômico e Geofísico, Universidade de São Paulo, Av. Miguel Stefano,* 4200, *CEP* 04301–970, *São Paulo, SP, Brazil*
[2] *Ministry of Scientific and Technical Research,* BP 4110, *Yaounde, Cameroon*

Accepted 1998 May 19. Received 1998 April 29; in original form 1997 April 30

SUMMARY

Measurement of samples from 154 sites in the continental sector of the Cameroon Volcanic Line yielded six palaeomagnetic poles, at 243.6°E, 84.6°N, $\alpha_{95} = 6.8°$; 224.3°E, 81.2°N, $\alpha_{95} = 8.4°$; 176.1°E, 82.0°N, $\alpha_{95} = 8.5°$; 164.3°E, 86.4°N, $\alpha_{95} = 3.4°$; 169.4°E, 82.6°N, $\alpha_{95} = 4.6°$ and 174.7°E, 72.8°N, $\alpha_{95} = 9.5°$, belonging to rocks which have been dated by the K–Ar method at 0.4–0.9 Ma, 2.6 Ma, 6.5–11 Ma, 12–17 Ma, 20–24 Ma and 28–31 Ma, respectively. The results are in general agreement with other palaeomagnetic poles from Oligocene to Recent formations in Africa.

The first three poles for rocks formed between 0.4 and 11 Ma are not significantly different from the present geographical pole. Together with other African poles for the same period, this suggests that the African continent has moved very little relative to the pole since 11 Ma. The other three poles for rocks dated between 12 and 31 Ma are significantly different from the present geographical pole, showing a 5° polar deviation from the present pole in the Miocene and 13° in the Middle Oligocene.

Key words: Cameroon, palaeomagnetism.

INTRODUCTION

From the Gulf of Guinea to the Adamawa Plateau there is a succession of major tectonic fractures aligned in an ENE–WSW direction, covered for most of its length by volcanic rocks, forming what is now called the continental sector of the Cameroon Volcanic Line (CVL). This CVL is a 1600 km Y-shaped chain of Tertiary to Recent generally alkaline volcanoes that extends more than 900 km across Cameroon from the Biu and Ngaoundere (Adamawa) plateaus to Mt Cameroon and Equatorial Guinea in the Gulf of Guinea (Fig. 1). It continues seawards for a further 700 km through the Atlantic islands of Principe, São Tomé and Pagalu.

This paper presents a detailed palaeomagnetic study of the continental sector of the CVL. Previous palaeomagnetic work on the CVL has been carried out by Piper & Richardson (1972), but was limited to rocks around Mt Cameroon and Bambouto from which a mean palaeomagnetic pole position was obtained at 121.1°E, 85.1°N and attributed to the Brunhes epoch.

TECTONIC SETTING

The CVL is partly superimposed upon a pre-existing fracture zone, the Central African Shear Zone, which cuts across a major post-Cretaceous uplift known as the Adamawa uplift, through southern Chad and the Central African Republic into western Sudan. To the north of the trend of Cameroon volcanic centres lies the Benue Trough, and to the south, the Foumban Shear Zone (Fig. 1), both of which are tectonic features with which the CVL is associated. The Foumban Shear Zone is a Precambrian structure which is considered to be the continuation of the Pernambuco lineament of Brazil prior to continental separation (Burke *et al.* 1971; Browne & Fairhead 1983; Gorini & Bryan 1976).

The Benue Trough of Nigeria is a 1000 km long depression that extends from the Niger Delta to Lake Chad, forming the major part of a 50–150 km wide NE–SW- trending sedimentary basin. The development of the rift system has been related to the differential opening of the Central and South Atlantic oceans, starting some 130 Myr ago when wrench fault zones extended from South America into the Gulf of Guinea and Africa, dissipating their strike-slip movement into extensional basins in Niger, Sudan and Kenya (Fairhead 1986, 1988; Benkhehil 1988). The CVL parallels the trough, and the similarity in shape and size of the two features led Fitton (1980, 1987) to suggest a model linking them to a common origin.

Burke *et al.* (1971), Browne & Fairhead (1983) and Moreau *et al.* (1977) link the CVL to the Foumban Shear Zone, which they think probably became reactivated to provide the conduit for magma to reach the surface, with the reactivation

* Now at: Unit for Geophysical and Volcanological Research, BP 370 Buea, Cameroon.

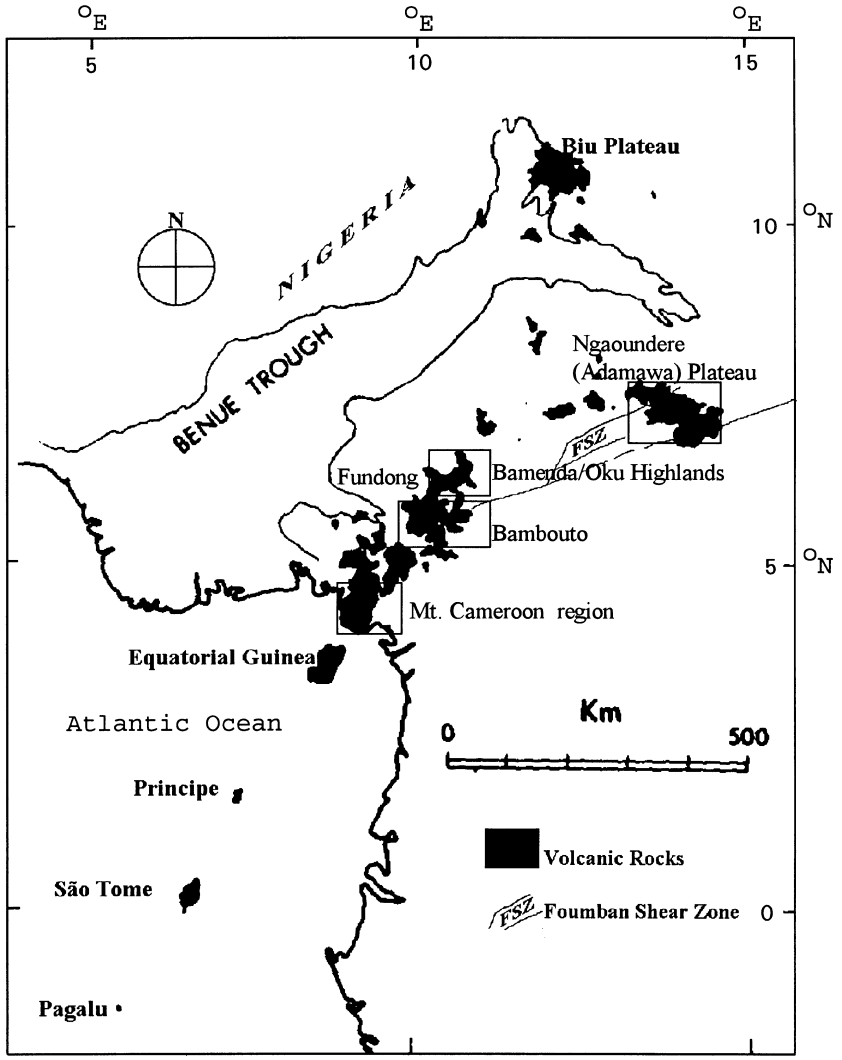

Figure 1. The Cameroon Volcanic Line and Benue Trough in West Africa. Rectangles indicate sampled regions.

generated by the continuous spreading of the South Atlantic (Mackenzie 1986).

GEOLOGY

This section summarizes the geology and geochronology of the main volcanic centres of the CVL, with the prime objective of establishing the links between them and the palaeomagnetic results. These volcanic centres include the Ngaoundere (Adamawa) plateau, the Bamenda Highlands, Mt Bambouto, Menengouba and Mt Cameroon (Fig. 1). Table 1 summarizes the available K–Ar ages for the volcanic centres. In general, K–Ar ages are considered minimum ages for volcanic rocks, representing the time since cooling below temperatures of argon retention in potassium-bearing minerals. Because of rapid cooling, K–Ar dates for volcanic rocks are essentially the age of crystallization. In most cases along the CVL, there is a concordance between K–Ar ages and stratigraphic position. The oldest-dated units in each of the volcanic centres are usually those lying unconformably on the crystalline basement. Trachytes and phonolite plugs which are frequently encountered as intrusions in the basalts present younger ages, and the young lavas of the recent craters and cones have the youngest ages. This goes some way to confirm the reliability of the datings. However, in the discussion that follows, sites with an age uncertainty greater than 1 Ma for periods later than the Oligocene have been left out. A detailed analysis of the geochronology data acquired in this project can be found in Marzoli 1996.

Ngaoundere (Adamawa) plateau

The volcanic complex of the Ngaoundere (Adamawa) plateau comprises a central volcano composed of alkaline basalts and basanites intruded by trachytes and phonolites (Temdjem 1986) with K–Ar ages between 6.5 and 11 Ma (Gouhier *et al.* 1974; Temdjem 1986). Two volcanic episodes in the region have been identified as:

(1) Upper Miocene—emplacement of large basaltic flows followed by trachyte intrusion;
(2) Quaternary—emission of pyroclastic material and formation of numerous cones and craters, most of which appear to be less than 0.9 Ma.

The upper Miocene flows have been largely altered to ferrallitic aluminous soils, more or less hardened to form

Table 1. Summary of available K–Ar ages for rocks of the Cameroon Volcanic Line. Asterisks indicate young cones and craters.

Region	Rock Type	K–Ar Age in Ma	Reference
Adamawa	Mugearite of Wakwa	*0.91 ± 0.2	Temdjem (1986)
(Ngaoundere)	Phonolite	6.5 and 6.8 ± 0.1	//
plateau	Hawaiite (Biskedje)	6.5 ± 0.2	
	Basanite	7.02 ± 0.2	Gouhier *et al.* (1974)
	Trachyte	7.9 and 9.8 ± 0.2	//
	Trachyte	9.26 ± 0.02	Marzoli (1996)
	10.61 ± 0.7	Temdjem (1986)	
Bambouto	Southwest flank	12.7–17.7	Tchoua (1974); Dunlop (1983) , Fitton & Dunlop (1985); Marzoli (1996).
	Pyroclastic flows of Ignimbrites in the northern flank and high plateaus	12.7–17.7	Tchoua (1974)
	Trachyte flows and domes	14.37–15.89	Tchoua (1974); Dunlop (1983).
	Extensive hawaiite lavas in the plateau	12.78–14.37	//
	Mugearite near Mbouda	20.95 and 20.75 ± 0.14	Marzoli (1996)
Manengouba	Recent basalts between Nkongsamba and Loum	*0.94 ± 0.06, 0.4 ± 0.04	Dunlop (1983)
Bamenda	1. Rhyolites and Basalts	28–31	Njilah (1991)
Highlands	2. Trachytes and basalts	22–24	Njilah (1991); Marzoli (1996).
	3. Basalt and hawaiites	14–18	Njilah (1991); Dunlop (1983).
	4. Recent basic flows	* < 1	Njilah (1991)
Mt Cameroon	Oldest lavas	9	Dunlop (1983)
	Young lava flows	* < 1	//
	Basalts Tiko Region	0.5 and 0.8	Hedberg (1968)
	Kumba crater	1.1–2.6 ± 0.2	Thouveny & Williamson (1988)

ferricretes. The acid lavas are extrusives that cut across the basement and basaltic flows. This volcanism, which is essentially phonolitic appearing in the form of domes, is still very fresh, indicative of their young age. Radiometric dating indicates that most of the domes were emplaced in the Quaternary (Temdjem 1986). They are aligned parallel to fractures that trend in the NW–SE direction.

Bamenda Highlands

The Bamenda Highlands include the Oku–Fundong massif and the numerous domes and plugs which overlook the town of Bamenda (Fig. 1). The rocks are composed principally of a spectrum of volcanic rocks that range in composition from primitive alkaline basalts to peralkaline rhyolite forming a bimodal alkaline basalt/trachyte/rhyolite suite. The highest points in the area are capped by a series of cinder cones and craters aligned NW–SE, some of which house lakes like Lake Nyos, Monoum and Lake Oku. The oldest volcanoes have been dated to range in age between 22 and 24 and 28–31 Ma (Njilah 1991; Marzoli 1996). Stratigraphically, four phases of magmatic activity can be identified:

(1) eruption of basalts in the first phase;
(2) successive intervals of ignimbrite emplacement;
(3) short periods of intensive production of trachytes; and
(4) renewed eruption of basalts in recent times, with the formation of numerous cinder cones and craters.

Mt Bambouto

The Bambouto mountain forms an elliptical cone with its long axis parallel to the CVL. Trachytes are the dominant rocks and form superimposed lava flows which terminate in cliffs. There also exist ash-flows, dykes and phonolite plugs. The central part of the volcano has collapsed into a horse-shoe-shaped crest caldera, where the trachytic and phonolitic plugs occur. The basal part of the mountain is composed mainly of basalts, which were later capped by trachytes and trachy-phonolites. Pre-caldera volcanic activity on the southwest flank of this volcano has been dated at 12.70 Ma to 17.17 Ma (Tchoua 1974; Dunlop 1983; Fitton & Dunlop 1985; Marzoli 1996). The various volcanic formations cover the slopes as well as high plateaus of the massif. These are exposed from the summit calderas in the north of the edifice right down to the region of Dschang in the south, where they lie on the Precambrian basement (Dumort 1968; Nyobe 1987; Nni & Nyobe 1995). They comprise large pyroclastic flows of ignimbrites (12.70–17.17 Ma, Tchoua 1974), huge trachyte flows, and extrusive domes whose ages vary between 14.37 and 15.89 Ma, and extensive hawaiite lavas in the plateaus dated at 12.78–14.37 Ma (Tchoua 1974; Dunlop 1983). The highest regions (above 1500 m) are mainly of differentiated lavas which are in some cases cross-cut by NE–SW veins of basanites and basalts. The emplacement of these veins represents the last phase of the precaldera volcanic activity (Nyobe 1987).

Mt Cameroon

Mt Cameroon (4075 m high) is a large volcanic horst which belongs to the CVL and is one of Africa's largest volcanoes. It is composed of alkaline basalts and basanites interbedded with small amounts of pyroclastic material (Fitton 1987). The lavas range in composition from almost aphyritic to strongly porphyritic types, with no lavas more developed than the hawaiites (Fitton 1987). Many recent volcanic cones found on the mountain are aligned SW–NE, as is the general morphology

of the massif. Fitton & Dunlop (1985) have given a K–Ar age of 9 Ma for the oldest basalt of Mt Cameroon, while Piper & Richardson (1972) have attributed the construction of the entire edifice of this mountain to Brunhes epoch times. This mountain is the only presently active volcano on the CVL, with six eruptions this century, the most recent being in 1982, and a volcanic gas explosion in 1989 (Ubangoh 1991).

SAMPLING

A total of 770 rock samples were collected from 154 sites in the major volcanic units on the CVL. The locations of sampled regions are indicated by rectangles in Fig. 1. An average of five orientated samples per site were collected from 142 of the 154 sites using a modified chain-saw motor to drill out cores, some being as long as 10 cm. Two or three orientated hand samples (blocks) were collected from the other 12 sites. An orientation stage with inclinometer, magnetic compass and solar compass was used for sample orientation. The magnetic compass reading was later corrected for mean declination at the site. When discrepancies occurred between azimuths determined by the solar and magnetic compasses, the azimuth determined by the solar compass was used. The sampling was done along road cuts and tracks.

LABORATORY METHODS

Several cores were taken from each of the blocks using an electric drill press in the laboratory. All the cores were sliced into one or two specimens (2.2 cm long), and their initial susceptibilities were measured using a susceptibility meter (Sapphire Instrument). A small powdered portion from a sample from each site was used for the determination of the Curie temperatures and hysteresis parameters. Polished sections were studied under the electron microscope to ascertain the oxidation states of the samples and determine the composition and grain sizes of the magnetic minerals. Analysis of measured magnetic parameters in combination with the electron microprobe analysis and demagnetization experiments indicated that more than 80 per cent of the samples bear a stable remanent magnetization (Ubangoh 1998).

An average of five specimens per site were used for palaeomagnetic measurements. The magnetometers used were the Cryogenic, Spinner (MS) and Schonstedt (DSM) magnetometers. Alternating field (a.f.) and thermal demagnetization experiments were performed on samples to isolate magnetic components and to test the stability of the remanent magnetization. The instruments used for a.f. demagnetization were a tumbling MOLSPIN—MS2 and the stationary-axis S1–4 (Sapphire Instruments). Thermal demagnetization was carried out with a Schonstedt TSD horizontal demagnetizer and changes in magnetic susceptibility were monitored with a Sapphire S1.

The demagnetization method for specimens was selected using two pilot specimens from each site: one was subjected to progressive demagnetization in an alternating magnetic field (a.f.) up to 100 mT, and the other to stepwise thermal cleaning up to 580 °C at intervals of 50 °C. The other specimens were submitted to at least six temperature or a.f. steps based on the results for the pilot specimens. For most specimens, the optimum temperatures and/or alternating fields were between 400 °C and 550 °C and 30 mT and 40 mT, respectively. Generally, specimens with very low initial intensities of magnetization (mostly from the acidic rocks) were demagnetized and measured in a cryogenic magnetometer, while those with low initial magnetic intensities were subjected to the conventional a.f. demagnetization method. High-coercivity specimens were treated with the thermal method. A combination of a.f. and thermal demagnetization was applied to specimens from sites whose pilot specimens indicated abnormally high initial intensities probably due to the action of lightning (Graham 1961). These were pre-treated with a.f. up to 15 mT and later thermally demagnetized.

Stereographic (Wulff) and orthogonal (Zijderverld 1967) projections were used to separate components of magnetization present in the specimens, and principal component analysis (Kirschvink 1980) was used to determine their directions. The directions thus obtained were averaged by site, and the statistical parameters were calculated assuming a Fisherian distribution.

RESULTS

In the great majority of the samples, apart from a viscous component which was removed at 150–200 °C in the thermally cleaned samples and at 5–15 mT in those demagnetized by a.f., the intensity of NRM decreased continuously while the direction of magnetization remained stable. Figs 2(a) and (b) show examples of the results of progressive thermal and a.f. demagnetizations. These generally revealed two NRM components. Thermal demagnetization up to 200 °C (Fig. 2a) removes a low-stability component of NRM directed towards the north with $I \approx -14^{\circ}$, which is similar to the direction of the present geomagnetic field in Cameroon. This low-stability component is interpreted as a secondary magnetization. For demagnetization temperatures above 200 to about 500 °C the trajectory of the vector end point is linear and trends toward the origin. This magnetization indicates no significant directional change in the 200–500 °C interval. The same directions were observed during the progressive demagnetization of the other specimens from this collection locality. In this case, the two components of NRM were sharply separated and the higher-stability component was taken as the characteristic magnetization of the rock.

Fig. 2(b) shows the result of progressive a.f. demagnetization for a representative basalt specimen. A.f. demagnetization to a peak field of 15 mT removes a small low-stability component similar in direction to that in Fig. 2(a) which is aligned in the direction of the present geomagnetic field in Cameroon. During the a.f. demagnetization to peak fields in the 15–70 mT interval, vector end points define a trajectory towards the origin. These observations indicate that the low-stability NRM component removed by a.f. demagnetization to 15 mT is a secondary magnetization, and it is assumed that the high-stability characteristic magnetization isolated above 15 mT is a primary TRM acquired during the original cooling of the CVL rocks. For the calculation of average direction per site, only directions defined by at least four points and with a maximum angular deviation (MAD) smaller than 10° were considered. The results are presented in Table 2 arranged in four groups depending on the location (volcanic centre) and age of the sites. Applying the significance test of Watson (1956), sites that are random at the 95 per cent confidence level are termed anomalous and have been omitted from subsequent analysis. The mean

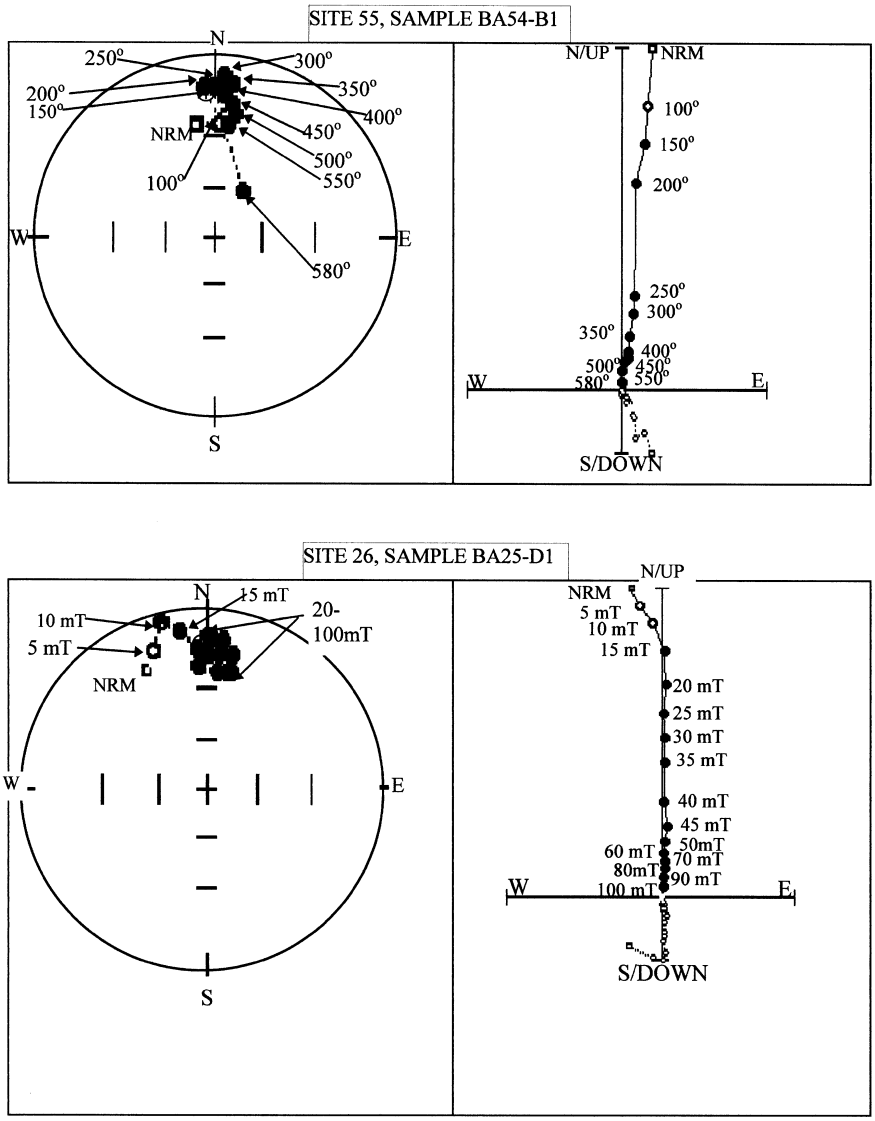

Figure 2. Example of stable magnetization behaviour for Cameroon Volcanic Line rocks. (a) A Wulff stereographic projection (open symbols: dips up, solid symbols: dips down) and Zijderveld diagram (open symbols: vertical-plane projections, solid symbols: horizontal-plane projections) for a thermally demagnetized specimen (BA 54-B1 from site 55). ⊕ represents the present geomagnetic field in Cameroon. (b) A Wulff stereographic projection and Zijderveld diagram for an a.f. demagnetized specimen (BA 25-D1 from site 26). Same symbols as for (a).

palaeomagnetic results for each of six different age groups are presented in Table 3 and will be discussed according to the different regions sampled and ages of the volcanic rocks.

Adamawa (Ngaoundere) plateau

The Ngaoundere rocks are considered in two volcanic groups, one belonging to the younger basalts dated at less than 1 Ma and the other to the older basalts and phonolites emplaced between 6.5 and 11 Ma. Both the younger and older formations contain samples with normal and reversed magnetization (Fig. 3a), confirming different phases of basalt flows and phonolitic intrusions. Close to 50 per cent of the sites in the older volcanic series fall into the anomalous category. This could be due to the abnormally high rate of alteration and bauxitization occurring in the region (Temdjem 1986), or the low content or very fine-grained nature of the magnetic minerals in the phonolites (Ubangoh 1998), thus resulting in a very low NRM, undetectable by the instruments employed. The large scatter in magnetic directions may be attributed to the tectonic process of uplift that has affected the region (Djoumani 1994). Although some of the younger series have been dated at 0.9 Ma, formations with normal magnetization are here assigned to the Brunhes epoch. After rotating the reverse directions through 180°, a mean palaeomagnetic direction and palaeomagnetic pole (No. 3 in Table 3) were calculated for the older series.

Bamenda Highlands

Two major geological age groups were sampled in this region. Group 1 samples are basalts and trachytes between Mbouda and Bamenda, around the town of Bamenda and in the Oku-Fundong region, with K–Ar ages found to be between 20 and 24 Ma (Table 1). Group 2 samples come from the oldest geological units (28–31 Ma) in the regions around Ndu and

Table 2. Site mean palaeomagnetic results for the Cameroon Volcanic Line.

			Site mean direction					VGPs		
S	Age (MA)	Nc/Nm	D (°)	I (°)	α95	k	R	(°) E	(°) N	Polarity
BA51	0.4–0.9	5/4	15	−6.3	5.7	183.9	3.978	131	72.70	N
BA54	//	4/3	26	−10.9	20.9	35.9	2.944	121	62.10	N
SW5	//	5/3	353	32.3	5.5	496.4	2.996	343	74.90	N
SW6	//	5/4	342	10.5	4.9	346.4	3.991	284	72.50	N
SW7	//	5/4	10.9	38.6	8.3	122.8	3.976	39	69.40	N
SW8	//	5/3	342	15.8	12	105.8	2.981	289	72.10	N
SW9	//	5/5	26.1	−39.6	8.7	78.2	4.949	146	53.20	N
SW10	//	3/3	339	15.8	16.1	59.6	2.967	291	69.20	N
SW11	//	5/4	338	−19	11.7	62.1	3.952	147	69.20	N
SW12	//	4/4	350	−8.5	6.9	179.7	3.983	238	64.20	N
SW13	//	5/4	353	−17.1	4.7	386.4	3.992	218	75.00	N
SW14	//	5/4	325	−0.1	12.6	54.3	3.945	273	55.00	N
SW16	//	5/4	348	−4	14.7	39.9	3.925	252	76.70	N
SW17	//	5/5	0.1	5.6	5.1	227.2	4.982	186	88.60	N
SW18	//	6/6	347	−11.7	4.2	257.2	5.981	242	73.30	N
SW19	//	5/3	354	20.2	9.1	186.3	2.989	325	81.40	N
SW13	//	5/4	3.6	−0.6	31.9	9.25	3.676	162	82.60	N
BA52	0.9	5/5	359	12.2	13.2	34.7	4.885	336	88.80	N
BA53	//	5/3	335	−33.4	52.4	6.6	2.697	236	56.00	N
CM81	//	3/3	0.8	0.7	12.7	96	2.979	187	83.10	N
CM82	//	5/4	350	13.9	14.2	42.5	2.989	285	80.70	N
CM83	//	4/4	179	3.1	36.1			198	81.30	R
CM84	//	4/3	348	51.1	49	7.3	2.726	351	63.10	N
CM85	//	5/5	183	−12.6	6.6	134.8	4.97	120	81.10	R
SW1	2.6	5/5	180	−18.8	6.2	280.5	4.974	5.6	85.50	R
SW2	//	5/5	174	12.8	5.3	209.7	4.981	35	77.00	R
SW3	//	5/4	352	−8.9	5	344.6	3.991	229	77.70	N
SW4	6.5	5/4	175	12.5	2.8	1052	3.997	214	77.70	R
CM99	//	5/4	181	−9	11.9	60.2	3.95	174	86.80	R
CM100	//	5/2	142	−22.7	42.2	37.1	1.973	293	52.10	R
CM92	7.9	4/3	104	72.5	19.2	42.2	2.953	45	1.40	/
CM93	//	5/2	223	37.3	13.5	343.1	1.997	139	41.70	/
CM94	//	3/2	106	54.6	51.8	25.4	1.961	246	8.90	/
CM95	//	5/4	258	30	17.2	29.6	3.899	121	9.30	/
CM86	8.22	5/4	179	12.1	5.7	258.6	3.988	216	75.80	R
CM87	//	5/3	20.9	−19.9	8.1	235.2	2.992	144	62.80	N
CM88	//	5/3	179	−16.9	8	223.7	2.989	332	88.00	R
CM89	//	4/3	345	−63	22.3	30.9	2.935	207	36.60	/
CM90	//	4/2	222	3.3	29	8.6	1.884	109	48.20	R
CM91	//	4/3	276	20.3	37.6	11.8	2.83	293	7.50	/
CM96	9.2	4/2	185	−65.1		57.6	1.983	19	50.00	R
CM97	//	5/4	78.7	42.7	16.5	31.8	3.906	80	13.30	/
CM98	//	4/3	80.1	41.2	51.2	6.8	2.705	81	12.00	/
CM101	11.4	5/3	3.8	−13.4	17.3	52	2.962	179	75.20	N
CM102	//	5/3	42.9	−25.6	10.4	150.7	2.986	130	42.60	/
CM103	//	5/3	344	8.4	9	189	2.991	275	74.00	N
BA14	14.8	5/5	31.9	52.9	14.8	27.54	4.855	54	49.90	N
BA15	//	5/3	312	9.5	4.7	676.6	2.997	281	42.40	/
BA17	//	5/3	138	9.9	12.4	99.8	2.98	267	46.70	/
BA18	//	5/2	225	1.4	19.2	17.4	1.994	118	44.10	/
BA48	//	5/4	12.8	−8.1	9.5	95.2	3.989	138	73.70	R
BA49	//	4/3	30	12.9	16.8	55.2	2.964	98	60.20	N
BA50	//	4/4	346	8	12.8	52.7	3.943	276	75.80	N
BA25	//	5/4	327	15.6	10.3	80.9	3.963	286	57.60	N
BA14	15.1	5/2	12.7	−0.6	39	41.4	1.976	125	76.10	N
BA18	//	5/3	132	27.9	53	6.7	2.701	256	38.00	/
BA19	//	5/4	22.1	29.5	6.7	190.4	3.984	73	66.10	N
BA20	//	5/2	198	9.5	73.5	13.8	1.927	129	69.10	R
BA26	//	6/6	352	−10.3	8.5	63.5	5.921	226	76.70	N
BA27	//	5/4	99.5	35.2	24.1	15.5	3.806	260	7.00	/
BA28	//	3/2	340	18.9	45	6.1	1.836	293	69.40	N
BA29	//	4/3	217	51	11.4	117.8	2.983	150	38.90	/
BA31	//	5/3	219	61.8	34.4	13.9	2.857	158	29.70	/
BA32	//	3/2	16.3	19.6	14.8	286.4	1.997	83	73.90	N

Table 2. (*Continued.*)

S	Age (MA)	Nc/Nm	Site mean direction D (°)	I (°)	α95	k	R	VGPs (°) E	(°) N	Polarity
BA33	//	4/2	352	−4.6	22.2	128.5	1.992	237	78.40	N
BA34	//	4/2	201	58.9	78.6	8.4	1.881	169	40.80	/
BA35	//	4/3	19	−1.3	13.9	80	2.975	118	70.10	N
BA36	//	6/5	332	−36.6	3.5	480.6	4.992	236	52.50	N
BA37	//	5/3	181	−5.6	33.3	14.8	2.863	180	87.20	R
BA38	//	5/3	174	0.5	15.6	63.4	2.969	237	81.70	R
BA39	//	5/3	231	−47.2	23.1	29.5	2.969	69	36.80	/
BA61	//	12/9	185	−25.6	11.9	19.6	8.592	42	80.40	R
BA62	//	4/3	291	54.2	3	1689	2.998	316	22.80	/
CM1	16.05	4/2	352	−8.3	42.3	37	1.273	230	77.40	N
CM2	//	4/2	13.6	−58	8.3	917.4	1.999	175	44.10	/
CM3	//	4/3	84.3	34.2	62.5	5	2.598	82	7.20	/
CM4	//	4/4	206	6.7	8.7	112.5	3.973	118	62.10	R
CM6	//	4/4	199	8.5	11.4	66.1	3.946	127	68.50	R
CM7	//	8/7	350	25.9	8.1	25.6	6.766	319	77.00	N
CM8	//	5/4	167	3.7	15	38.4	3.922	251	74.80	R
CM9	//	5/3	166	4.1	8.7	200.4	2.99	252	74.10	R
CM10	//	5/2	158	−11.3	74	13.4	1.925	281	68.00	R
CM11	//	6/6	3.9	−26	11.4	35.3	5.858	179	70.30	N
CM12	//	5/2	179	−6.5	17.3	210.5	1.995	211	87.40	R
CM15	//	4/3	350	−14.1	7.2	292.7	2.993	230	73.60	N
CM16	//	4/3	4.9	−4	5.5	507.1	2.996	157	81.10	N
CM17	//	3/2	346	−9	10.3	590.5	1.998	245	72.70	N
CM20	//	3/2	198	9.5	73.5	13.8	1.927	129	69.10	R
CM21	//	3/3	345	−12.2	6.8	327.8	2.994	243	70.80	N
CM22	//	3/2	303	49.4	31.9	63.5	1.984	312	31.20	/
CM23	//	3/2	4.5	5.5	22.7	122.7	1.992	161	80.60	N
CM25	//	5/4	327	15.6	10.3	80.9	3.963	286	57.60	N
CM40	20.9	5/3	1.3	−57.8	20.5	37.3	2.946	189	46.00	/
CM41	//	5/3	16.4	24.7	11.9	107.7	2.981	75	72.30	N
CM42	//	5/4	358	24.2	7.6	145.3	3.979	357	82.80	N
CM43	//	5/4	73.2	7.7	29.9	72	1.986	98	17.10	/
BA2	20.1	5/4	190	−25.5	15	37.37	3.92	62	77.90	R
BA4	//	5/3	358	−5.1	15.8	61.4	2.963	206	81.20	N
CM44	//	5/4	338	−19.2	15.6	35.68	3.915	245	63.20	N
CM45	//	5/3	151	47.4	38.2	11.5	2.825	228	45.50	/
CM46	//	5/3	17.6	7.5	22.9	30	2.933	106	72.40	N
CM47	//	5/2	6.4	−14.3	44	33.3	1.97	164	75.50	N
CM48	//	5/4	349	−15.8	9.4	95.8	3.969	229	72.10	N
CM49	//	5/3	351	−4	14.3	74.9	2.973	241	77.80	N
CM50	//	5/3	98.1	10.3	29.8	274	7.40	/		
CM51	//	5/4	276	27.6	28.9	10.4	3.713	294	7.40	/
CM52	//	5/4	176	7.8	7.3	159.8	3.981	210	79.60	R
CM54	//	5/5	186	−35	7.8	97.6	4.959	28	75.30	R
CM55	//	6/6	181	−37.3	12.5	26.4	5.803	15	74.40	R
CM56	//	6/6	72.4	−24.1	8.4	65.3	5.923	115	15.90	/
CM57	//	6/5	186	−37.2	12.1	40.9	4.902	30	73.60	R
CM58	//	2/2	303	7.5	70			281	33.30	/
CM59	//	2/2	261	46.7	3.6	530	1.998	129	5.60	/
CM63	//	2/2	161	−13.2	25.2			286	70.90	R
CM64	//	4/3	344	−11	4.5	739.3	2.999	248	70.40	N
BA11	23.3	4/4	43	−6.4	24.8	26.4	2.924	112	46.10	/
BA31	//	4/3	2	−21.4	35.2			184	72.60	N
BA43	//	4/2	196	−2.9	5	2529	2	123	77.50	R
BA56	//	4/3	152	−38.2	63	2.3	2.115	313	58.70	/
BA57	//	2/2	27.7	−65.3	35.9	5.7	1.826	168	31.50	/
BA58	//	4/4	126	−14.9	22.1	18.2	3.835	285	35.90	/
BA59	//	4/4	33.9	−13.6	13.7	128.5	3.935	120	53.90	N
BA60	//	4/3	141	16.4	23.7	499.5	2.929	260	49.00	/
BA61	//	4/3	356	−16.5	35	13.4	2.851	208	75.00	N
BA62	//	5/4	9.4	−8	18	43	2.993	146	76.20	N
BA63	//	5/5	50.3	2.5	10	59.7	4.933	103	39.70	/
BA6	23	5/3	357	−3.6	7	301.2	2.993	209	81.70	N
BA8	//	5/3	258	19.7	19.7	40.2	2.95	112	11.10	/

Table 2. (*Continued.*)

S	Age (MA)	Nc/Nm	Site mean direction D (°)	I (°)	α95	k	R	VGPs (°) E	(°) N	Polarity
BA9	//	5/2	268	5.3	37.9	45.5	1.978	104	4.00	/
BA10	//	5/5	195	16.8	7.2	107	4.963	145	68.80	R
BA12	//	5/4	155	−12.6	18	17.2	3.826	283	64.90	R
BA22	//	5/4	196	−3.9	14.3	42.2	3.929	117	73.80	R
BA32	//	5/2	7	7.9	71			174	87.60	N
BA33	//	6/6	346	1.7	7.8	75.4	5.934	255	74.00	N
BA37	//	3/2	193	12.2	76.8	3.668	2.454	145	72.10	R
BA38	//	5/4	354	0.2	8.3	122.7	3.976	236	81.30	N
BA3	28	5/3	190	32	18	46.6	2.957	167	64.40	R
BA5	//	5/3	283	31.4	10	213	2.993	298	14.40	/
BA24	//	6/6	151	51.2	22.3	8.8	5.435	225	42.70	/
BA25	//	5/3	260	9.5	12.1	105.5	2.981	107	9.10	/
BA26	//	5/3	110	3.9	21.3	34.6	2.987	276	19.70	/
BA27	//	5/2	294	−20.5	29	76.5	1.987	266	21.80	/
BA28	//	2/2	198	32.2	65	22	1.955	174	60.50	R
BA29	//	3/3	22.2	−43.8	69	15.2	1.955	157	51.50	N
BA39	//	4/3	347	4	10	152	2.987	263	76.40	N
BA40	//	5/5	34.1	−8.9	16.5			117	54.30	N
BA41	//	5/4	176	22.1	9.5	95.2	3.969	24	71.70	R
BA42	//	5/4	202	2.4	17.4	29	3.897	119	67.00	R
BA46	//	5/5	161	28.1	19.5	16.28	4.754	233	61.30	R
BA47	//	5/4	12.1	−10.7	4.4	439.7	3.993	144	73.40	N
BA19	31	5/4	25.9	14.3	19.7	10.2	3.714	97	64.30	N
BA44	//	5/4	21.5	−17.4	30.8	9.4	2.99	135	63.80	N
BA45	//	5/3	184	37	8.9	191	2.99	182	62.80	R

S = Site number (SW1–19: Mt Cameroon region; CM1–64: Bambouto region; CM81–103: Ngaoundere region; BA1–63: Bamenda highlands and Loum); Nc/Nm = number of collected samples per site/number of samples used for mean determination; D and I = declination and inclination of the characteristic remanent magnetization, respectively; k and α_{95} = Fisher's precision parameter; R = resultant of Nm unit vector; VGP = Virtual Geomagnetic Pole, α_{95} is semiangle of cone of 95 per cent confidence about mean direction, N = Normal, R = Reverse, / = odd.

Table 3. Mean palaeomagnetic results for Cameroon Volcanic Line.

Locality	Age (Ma)	N	Direction of magnetization D (°)	I (°)	R	k	α_{95}(°)	Palaeomagnetic pole position LONG. (°)E	LAT. (°)N	A_{95}(°)
1. Mt Cameroon, Loum, Ngaoundere	0–0.9	25	352.7	2.5	24.64	18.4	7.9	243.6	84.6	6.8
2. Kumba	2.6	4	354.9	−4.4	3.97	112.7	8.7	224.3	81.2	8.4
3. Ngaoundere	6.5–11	8	5.2	−6.3	7.83	52.1	9.1	176.1	82.0	8.5
4. Bambouto	12–17	33	358.2	1.5	31.88	27	6.3	164.3	86.4	3.4
5. Bamenda—Oku	20–24	26	1.6	−2.3	25.36	38.9	6.3	169.4	82.6	4.6
6. Bamenda—Oku	28–31	13	19.6	−3.5	11.5	21.8	9.8	174.7	72.8	9.5

N = number of sites; α_{95} = semiangle of cone of 95 per cent confidence about mean direction; k = Fisher's precision parameter; R = resultant vector; A_{95} (°) = semiangle of cone of 95 per cent confidence about the pole position.

Foundong. The two groups contain both normal and reversed directions (Fig. 3b). The antipole of the mean of the reversed-polarity sites is within 3° of the mean of the normal-polarity sites. This suggests that the characteristic directions are free of secondary NRM and that the time sampling afforded by this set of palaeomagnetic data has adequately averaged geomagnetic secular variation. It also confirms the efficiency of the demagnetizing processes. Omitting the anomalous sites and rotating the reversed directions by 180°, combined mean directions and mean pole positions (Table 3, nos 5 and 6) were calculated for the two age groups.

Mt Bambouto

Palaeomagnetic sites around Mt Bambouto show normal and reversed directions consistent with the many volcanic phases registered in the region that have K–Ar ages between 12.7 and 17.17 Ma. The normal and reversed directions are antipodal (Fig. 3c), with the antipole of the mean of the reversed-polarity sites within 2° of the mean of the normal-polarity sites. These combine to give a mean magnetization direction of $D = 358.2°$, $I = 1.5°$ ($\alpha_{95} = 6.3°$, $k = 27.0$, $N = 33$) and a mean pole at 164.3°E, 86.4°N.

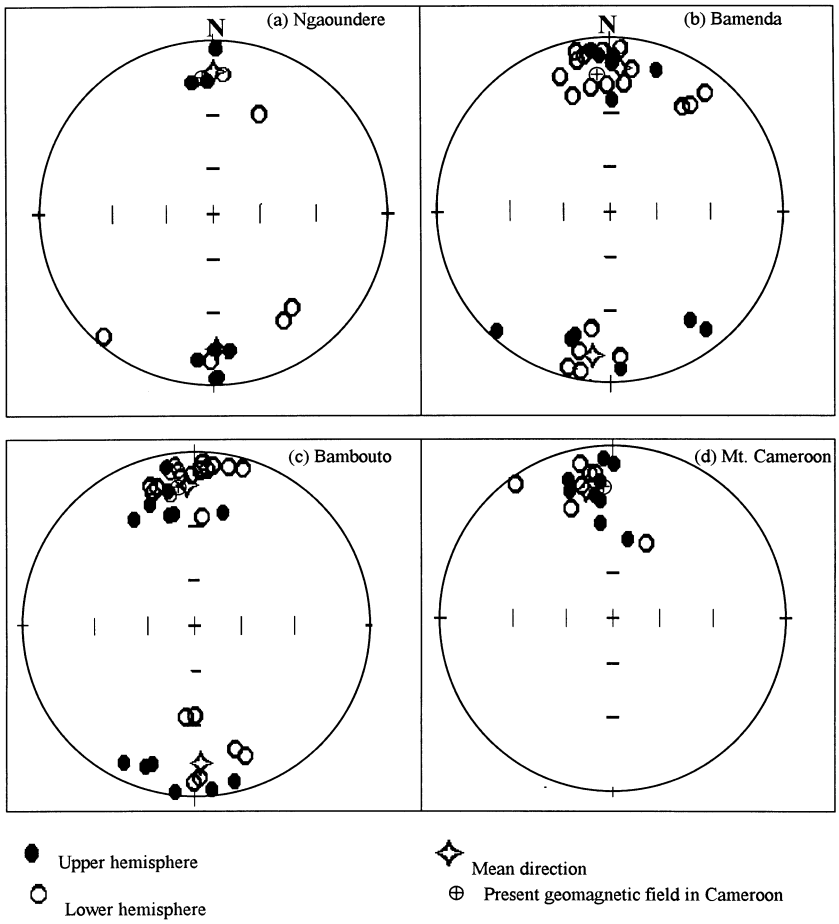

Figure 3. Site mean magnetization directions for the different volcanic centres of the Cameroon Volcanic Line: (a) Ngaoundere (Adamawa) plateau, (b) Bamenda, (c) Bambouto, (d) Mt Cameroon. Open and solid symbols refer to up and down dips, respectively. ⊕ represents the present geomagnetic field in Cameroon.

Four sites studied between Kekem and Loum to the south of Bambouto and close to Mt Manengouba give a mean direction of $D = 7.8°$, $I = 5.7°$ ($\alpha_{95} = 19.0°$, $N = 4$). Rocks of this region have been dated by Fitton & Dunlop (1985) at 0.4 ± 0.04 and 0.9 ± 0.04 Ma. The four sites, however, are all normally magnetized and so are assigned an age of 0.4 ± 0.04 Ma based on the polarity column of the geological timescale.

Mt Cameroon

13 of the 15 sites sampled on the flanks of Mt Cameroon starting from the shore of the Atlantic Ocean in Limbe and from the limit of the sedimentary basin in Muyuka combine to give a mean direction of $D = 357.5°$, $I = 5.8°$, $\alpha_{95} = 8.2°$, $k = 17.8$, $N = 13$). They are all normally magnetized (Fig. 3d). Considering that the Tiko region from which ages of 0.5 and 0.8 Ma have been reported (Hedberg 1968) is at the foot of the mountain close to Limbe and that this volcanic mountain has continued to be active up to Recent times, the normality of the directions in the Mt Cameroon samples implies that this volcano was emplaced in the Brunhes epoch. A mean Holocene direction has been calculated (Table 3, no. 1) by combining the directions from the recent volcanic rocks of Ngaoundere, Loum and Mt Cameroon.

Four sites taken from young basalts in the northeast of Mt Cameroon between Kumba and Ngute show two normal and two reversed directions which are antipolar. Thouveny & Williamson (1988) have reported ages of 1.1 and 2.6 ± 0.2 Ma for the Barombi crater in Kumba. From field relations between the sites and the crater, the upper limit of this age can be assigned to the four sites. Combining the directions after normalization of the reversed directions gives the mean direction and pole indicated in Table 3 as no. 2.

DISCUSSION AND CONCLUSIONS

The basic result of this investigation is the determination of six new palaeomagnetic poles for the African continent (Table 4), five of which pass the minimum reliability criteria of Besse & Courtillot (1988); namely, at least six sites and 36 samples, a 95 per cent confidence interval less than 10° in the Cenozoic, successive demagnetization, and a small dating uncertainty (1 Ma is considered here as the maximum uncertainty for periods after the Oligocene).

Pole 1 (M1 in Table 4) is obtained from 25 sites on the recent basalts (<1 Ma old) around Mt Cameroon, Loum and the Ngaoundere plateau. The palaeomagnetic pole position is also shown in Fig. 4(a) as M1, along with a selection of African palaeomagnetic poles determined for the period ranging from

Table 4. Selection of palaeomagnetic data from Africa during the Tertiary.

Pole	Locality	Age (Ma)	N	K	A_{95} (°)	Palaeomagnetic Pole Position Long. (°E)	Lat. (°N)	Reference
M1	Mt Cameroon, Loum & Ngaoundere plateau	0.6–0.9	25	18.4	6.8	243.6	84.6	Present study
M2	Kumba	2.6	4	112.7	8.4	224.3	81.2	Present study
P3	Equatorial Guinea	Bruhnes epoch	52	206.8	4.5	189.0	85	Piper & Richardson (1972)
P4	São Tomé	//	49	192.9	4.8	199.4	86.4	//
P5	Nigerian volcanics	1.4	4	200	6.5	239.6	80	Marton & Marton (1976)
P6	Afar Depr, Ethiopia	Bruhnes epoch	24	19.2	5.1	254.7	88	Harrison *et al.* (1977)
P7	Huruj As Volc, Libya	0.4–2.2	27	14	8.5	171	83	Ade Hall *et al.* (1974)
P8	Afar Volc, Djiboutti	Holocene	7		10	253	82	Pouchan & Roche (1971)
P10	Volcanics, Kenya	1.6–6.9	161	5.9	3.9	296.6	83.9	Patel & Raja (1979)
P11	Garian Volc, Libya	2.1–6.1	23	35	6.7	123	88	Ade-Hall *et al.* (1975)
P12	Jebel Soda, Libya	Miocene, Pliocene	12	23.5	7.4	196.1	79.4	Schult & Soffel (1973)
P13	Rift Valley lavas	0–7	120	22	2.1	149.7	88	Reilly (1970)
Mn	Mean African pole	Pliocene—Recent	13	271.2	2.8	219.1	85.8	Present paper
M3	Ngaoundere Plateau	6.5–11	8	52.1	8.5	176.3	82.0	Present paper
P15	Morocco Lavas	5–13	18	35.7	6.4	161	85.8	Najid *et al.* (1981)
P16	Jebel Soda, Libya	10–12	12	23.5	7.4	196.1	78.4	Ade-Hall *et al.* (1975)
P17	Kenya & Tanzania	Upper Neogene	22	13.4	6.1	186.6	86.6	Reilly *et al.* (1976)
M4	Bambouto	12.- 17	33	27.0	3.4	164.3	86.4	Present paper
P19	Cape Verde	Middle Miocene		1.6	3.5	136.6	85.2	Watkins *et al.* (1968)
P20	Kenya	//		24	5.2	188	87.4	Raja (1968)
M5	Bamenda-Oku	20–24	26	38.9	4.6	169.4	82.6	Present paper
P22	Turkana lavas, Kenya	14–23	62	35.3	2.3	163.3	84.6	Reilly *et al.* (1976)
M6	Bamenda-Oku	28–31	13	21.8	9.5	174.7	72.8	Present paper
P26	Ethiopia	30.7–36.3	22	14.4	6.4	170.3	75.3	Schult (1974)
P27	//	49 ± 15	20	34.9	4.3	168.0	80.8	Brock *et al.* (1970)

N = Number of sites; A_{95} = Semiangle of cone of 95 per cent confidence; K = Fisher's precision parameter; M = poles determined in this paper for the Cameroon Volcanic Line; Mn = mean African palaeomagnetic pole calculated for periods younger than the Miocene; P = other African palaeomagnetic results from previous studies.

Pliocene to Recent. As can be seen in Fig. 4(a), the Cameroon palaeomagnetic pole determined in this paper is not significantly different from the pole position found by Piper & Richardson (1972) for young volcanic materials of the same age in the oceanic sector of the CVL (Equatorial Guinea and São Tomé). They are all on the side of the geographical pole farthest from the sampling site. Wilson (1970) has explained the displacement of the palaeomagnetic poles for the Upper Tertiary times to the far side of the globe to the sampling site in terms of an off-centre displacement of the effective dipole source. The statistical oval of confidence at the 95 per cent level for the Cameroon pole, unlike that of São Tomé, includes the present rotation pole, as expected for rocks of this age. This is a good indication that the magnetic field had approximated to a geocentric axial dipole field during the emplacement of the Mt Cameroon basalts and that secular variation was averaged out. A 95 per cent circle of confidence that includes the geographical pole is in agreement with the observations by Cox & Doell (1960), Irving (1964), Opdyke & Henry (1969) and Isaacson & Heinrich (1976) that the mean poles for the Upper Tertiary to Recent are very close to the geographical pole. The three CVL poles, like the majority of the other Pliocene–Recent palaeomagnetic poles from Africa, are located on a side of the geographical pole not very different from the one obtained by Piper & Richardson (1972) for Cameroon volcanic rocks (shown in Fig. 4a as PR) with circles of confidence that overlap. The small difference could be attributed to the fact that, in determining their pole, Piper & Richardson did not take into consideration the age differences among the sampled Cameroon rocks (< 1 Ma–31 Ma).

Pole 2 (M2 in Table 4 and Fig. 4) is derived from only four sites close to Kumba. The rocks formed some 2.6 Myr ago. The number of sites does not meet the minimum reliability criteria, although pole 2 is not significantly different from pole 1 and from the present geomagnetic pole.

Eight sites from the older volcanic rocks in the Ngaoundere plateau (Fig. 1), which have been dated by many authors (Table 1) to have K–Ar ages between 6.5 and 11 Ma, combine to give Pole 3. This pole is presented in the second part of Table 4 and in Fig. 4(b), along with two other African poles in the same age range. These four Upper Miocene African poles are in good agreement with each other and present overlapping circles of confidence that include the geographical pole. This indicates that the African continent has moved little relative to the geographical pole over the last 11 Ma.

Pole 4 (M4 in Table 4) is a very good Middle Miocene pole with a small circle of confidence derived from 33 sites belonging to the trachytes and basalts around Mt Bambouto. Rocks in this area have been dated by many authors to have K–Ar ages between 12 and 17 Ma (Table 1). The pole is in good agreement with the Miocene pole determined for Cape Verde Island by Watkins *et al.* (1968), who found a palaeomagnetic pole for lavas of this island at 136.6°E, 85.2°N with an α_{95} of 3.5°. The result is also not significantly different from the pole obtained for the Miocene Central rift lavas of Kenya (Raja 1968) found at 188.0°E, 87.4°N with a circle of confidence of 5.2°. These

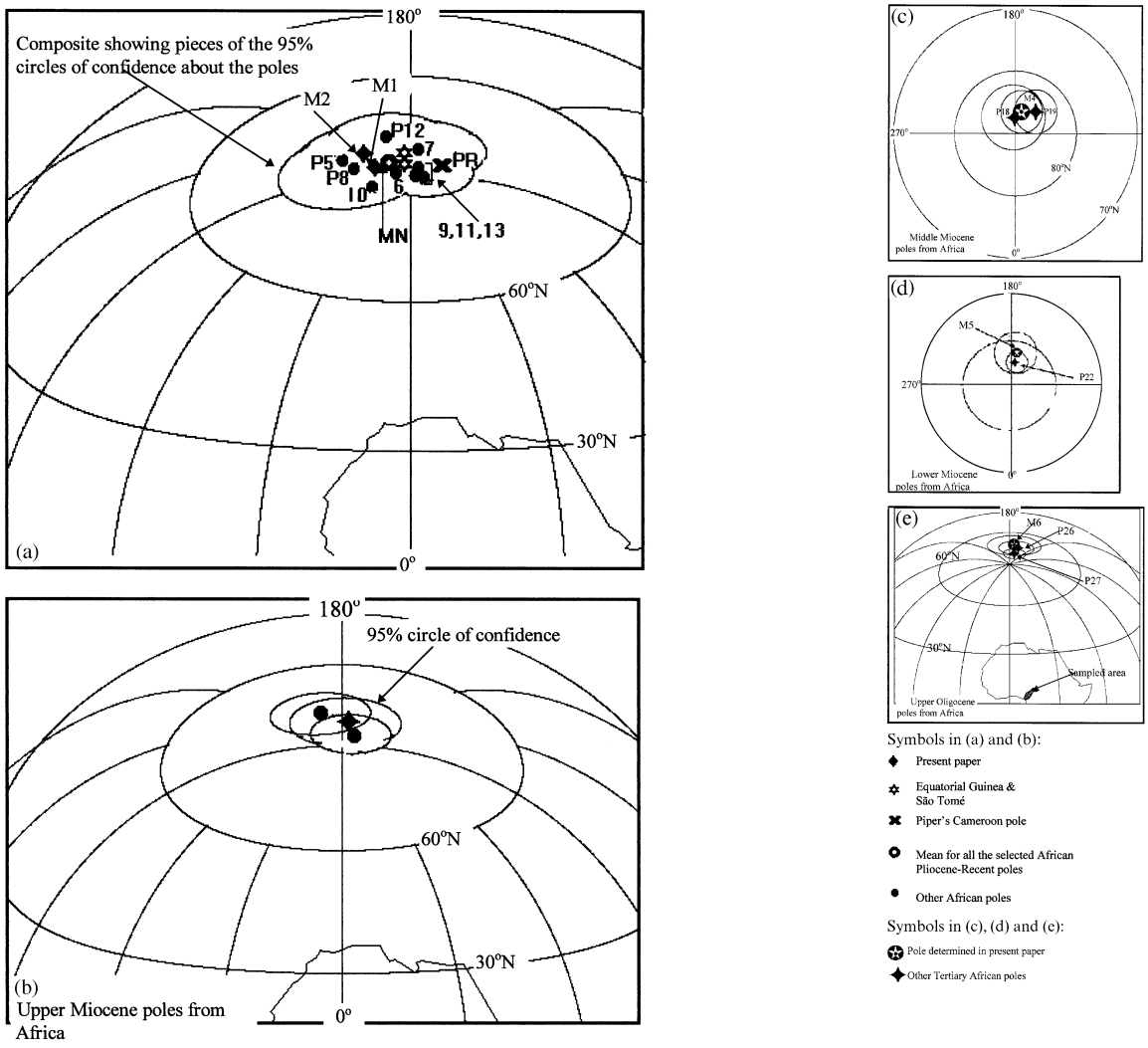

Figure 4. Tertiary palaeomagnetic pole positions from the African continent: (a) Pliocene to Recent poles; (b) Upper Miocene poles; (c) Middle Miocene poles; (d) Lower Miocene poles; and (e) Middle Oligocene poles. (See Table 4 for references.)

poles (Fig. 4c) are slightly different (4° deviation) from the present geographical pole, thus indicating a polar movement for Africa since the Middle Miocene.

For older periods, pole 5 (M5 in Table 4) has been obtained from the lavas of the Bamenda–Oku highlands that have K–Ar ages between 20 and 24 Ma (Table 1). The palaeomagnetic pole is given in Table 4 and plotted in Fig. 4(d) along with one other African Lower Miocene palaeomagnetic pole determined from the volcanic rocks of Kenya and Tanzania (Table 4) by Reilly *et al.* (1976). The three poles closely agree and are significantly different from the present geographical pole, indicating a polar shift of about 6° since the Upper Oligocene–Lower Miocene.

Pole 6 (M6 in Table 4) has been successfully isolated for the Middle Oligocene CVL rocks. This is from 13 sites sampled on the oldest volcanic rocks dated in the Oku region by Njilah (1991) at 28–31 Ma. The determined pole is plotted in Fig. 4(e) along with a 30.7–36.3 Ma palaeomagnetic pole determined for the plateau volcanics of Ethiopia by Schult (1974) at 170.3°E, 75.3°N with an α_{95} of 6.4°, and another (49 ± 15 Ma) determined for the Ethiopia Flood basalts by Brock *et al.* (1970) at 168°E, 80.8°N, $\alpha_{95} = 4.3°$. The three poles are in good agreement with each other, with their circles of confidence intersecting. If we consider the lower age limit for the pole of Brock *et al.* (1970), the three poles can be conveniently averaged.

Taking the results together with those for poles 4 and 5 confirms the suggestion of Brock *et al.* (1970) that the polar wander path for Africa shows a 5° polar deviation from the present pole in the Miocene, which is enlarged to about 13° in the Middle Oligocene.

In conclusion, this study has provided six new Tertiary poles for the African continent which are in agreement with other African poles for the same period. Although the circles of confidence of the poles older than Pliocene overlap, they do not include the geographical pole. There is a significant polar difference of $\approx 5°$–13° between Upper Miocene and Middle Oligocene poles.

ACKNOWLEDGMENTS

Many thanks go to Professors Melfi, Piccirillo and Trompet, Drs Montes-Lauar, Nni and Marzoli, and Messrs Aka, Aduraman, Mbaraga and Ngyimapi for assisting in the field

work, and to Professor Marcia Ernesto for co-ordinating the project. The funding was provided by FINEP/PADCT Brazil and the Ministry of Scientific and Technical Research Cameroon.

REFERENCES

Ade-Hall, J.M., Gerstein, S., Gerstein, R., Reynolds, P., Dagley, P., Mussett, A. & Hubbard, T., 1975a. Geophysical studies of North African Cenozoic volcanic areas: III. Garian, Libya, *J. Earth Sci.,* **12,** 1264–1271.

Ade-Hall, J.M., Reynolds, P.H., Dagley, P., Mussett, A.E. & Hubbard, T.P., 1975b. Geophysical studies of North African Cenozoic volcanic areas: II. Jebel Soda, Libya, *J. Earth Sci.,* **12,** 1257–1263.

Ade-Hall, J.M., Reynolds, P.H., Dagley, P., Mussett, A.E., Hubbard, T.P. & Klitzsch, F., 1974. Geophysical studies of North African Cenozoic volcanic areas: I. Haruj Assuad, Libya, *J. Earth Sci.,* **11,** 998–1006.

Benkhelil, J., 1988. Structure et evolution geodynamique du intra-continentale de la Benue (Nigeria), *Bull. Centre Rech. Explor. Prod Elf-Aquitaine,* **12,** 315–321.

Besse, J. & Courtilot, V., 1988. Paleogeographic maps of the continents bordering the Indian Ocean since the Early Jurassic, *J. geophys. Res.,* **93,** 11 791–11 808.

Brock, A., Gilson, I.L. & Gacci, P., 1970. The paleomagnetism of the Ethopian flood basalt succession near Addis Ababa, *Geophys. J. R. astr. Soc.,* **19,** 484.

Browne, M.A. & Fairhead, J.D., 1983. Gravity study of the Central African rift system: A model of continental disruption. 1. Ngaoundere Abu Gabra Rifts, *Tectonophysics,* **94,** 187–202.

Burke, K.C., Desauvagie, T.F.J. & Whiteman, A.J., 1971. Opening of the Gulf of Guinea: Geological History of the Benue Depressão and Niger Delta, *Nature,* **233,** 51–55.

Cox, A. & R. Doell, R., 1960. Review of paleomagnetism, *Geol. Soc. Am. Bull.,* **71,** 645–768.

Djoumani, P.Y.H., 1994. Apport de la gravimétrie à l'étude de la lithosphere continentale et implications geodynamiques: étude d'un bombement intraplaque—le massive de l'Adamauao (Cameroun), *PhD thesis,* Université de Paris-Sud, France.

Dumort, J.C., 1968. Notice Explicative de la Feuille Douala Ouest aveccarte gélogique au 1/500 000, Dir. Mines Géol., Cameroon.

Dunlop, M.H., 1983. Strontium isotope geochemistry and Potassium–Argon studies on volcanic rocks from the Cameroon Volcanic Line, West Africa, *PhD thesis*, University of Edinburgh, UK.

Fairhead, J.D., 1986. Geophysical controls on sedimentation in the African rift systems, in *Sedimentation in the West and Central African Rift System,* eds Frastick, A.T. *et al.,* Geological Society Special Publication, **23,** 19–27.

Fairhead, J.D., 1988. Mesozoic plate tectonic reconstructions of the Central South Atlantic Ocean. The role of the West and Central African rift systems, *Tectonophysics,* **155,** 181–191.

Fitton, J.G., 1980. The Benue trough and the Cameroon line. A migrating riftsystem in west Africa, *Earth planet. Sci. Lett.,* **51,** 132–138.

Fitton, J.G., 1987. The Cameroon line west Africa: a comparison between oceanic and continental alkaline volcanism, alkaline igneous rocks, *Geological Soc. Spec. Pub.,* **30,** 273–291.

Fitton, J.G. & Dunlop, H.M., 1985. The Cameroon Line, West Africa, and its bearing on the origin of oceanic and continetal alkali-basalt, *Earth planet Sci. Lett.,* **72,** 23–38.

Gorini, M.A. & Bryan, G.M., 1976. The tectonic fabric of the equatorial and adjoining continental margins: Gulf of Guinea to Northern Brazil, *An. Acad. Bras. Sci.,* **48** (Suppl.), 101–119.

Gouhier, J., Nougier & Nougier, D., 1974. Contribution a l'étude Volcanologique du Cameroun ('Ligne du Cameroon'-Adamawa), *Ann. Fac. Sci. Cameroun,* **17,** 28–36.

Graham, K.W.T., 1961. The remagnetization of a surface outcrop by lightning currents, *Geophys. J. R. astr. Soc.,* **6,** 85–91.

Harrison, C.G.A., Stieltjes, L. & Tarasiewicz, E., 1977. Paleomagnetism of samples from the axial zone of the Afar depression, *Earth planet. Sci. Lett.,* **34,** 273–283.

Hedberg, J., 1968. A geological analysis of the Cameroon trend, *PhD thesis,* University of Princeton, NJ.

Irving, E., 1964. Palaeomagnetism and its Application to Geologial and Geophysical Problems, John Wiley, New York.

Isaacson, L.B. & Heinrichs, D.F., 1976. Paleomagnetism and secular variation of Easter Island Basalts, *J. geophys. Res.,* **81,** 1476–1481.

Kirschvink, J.L., 1980. The least-squares line and plane and the analysis of palaeomagnetic data, *Geophys. J. R. astr. Soc.,* **62,** 699–718.

Mackenzie, D., 1986. Geology of Cameroon's gas catastrophe, *New Scientist,* 26–27

Marton, E. & Marton, P., 1976. A paleomagnetic study of the Nigerian volcanic province, *Pure appl. Geophys.,* **114,** 61–69.

Marzoli, A., 1996. Il Magmatismo del sectore continentale della Linea Volcanica del Cameroon, *PhD thesis,* Universita Degli Studi Di Trieste, Italy.

Moreau, C., Regnould, J.M., Deruelle, B. & Robinson, B., 1977. A tectonic model for the Cameroon Line, Central Africa, *Tectonophysics,* **139,** 317–334.

Najid, D., Westphal, M. & Hernandez, J., 1981. Paleomagnetism of Quaternary and Miocene lavas from North-East and Central Morocco, *J. Geophys,* **49,** 149–152.

Njilah, J.K., 1991. Geochemistry and Petrogenesis of Tertiary Quaternary Volcanic rocks from the Oku-Ndu Area, N.W. Cameroon, *PhD thesis,* University of Leeds, UK.

Nni, J. & Nyobe, J.B., 1995. Géologie et pétrologie des laves pre-caldériques des mounts Bambouto: Ligne du Cameroun, *Geochim. Brasil.,* **9** (1), 47–59.

Nyobe, J.B., 1987. A geological and geochemical study of the Fongo-Tongo related bauxite deposits—Western Highlands. Republic of Cameroon, *PhD thesis,* University of Lehigh, USA.

Opdyke, N.D. & Henry, K., 1969. A test of the dipole hypothesis, *Earth planet. Sci. Lett.,* **6,** 139–151.

Patel, J.P. & Raja, P.K.S., 1979. Paleomagnetic results from the Narosura and Magadi Volcanics of Kenya, *Phys. Earth planet. Inter.,* **19,** P7–P14.

Piper, J.D.A. & Richardson, A., 1972. The paleomagnetism of the Gulf of Guinea volcanic province, West Africa, *Geophys. J. R. astr. Soc.,* **29,** 147–171.

Pouchan, P. & Roche, A., 1971. Etude paleomagnetique de formations volcaniques du Territoire des Afars et Issas, *C. R. Acad. Sci. Paris Ser. D,* **272,** 531–534.

Raja, P.K.S., 1968. A paleomagnetic study of some East African rocks, *PhD thesis,* University of London, UK.

Reilly, T.A., 1970. Some paleomagnetic results from central east Africa and the Seychelles Islands, *PhD thesis,* University of London, UK.

Reilly, T.A., Raja, P.K.S., Mussett, A.E. & Brock, A., 1976. The palaeomagnetism of Late Cenozoic Volcanic rocks from Kenya and Tanzania, *Geophys. J. R. astr. Soc.,* **45**, 483–494.

Schult, A., 1974. Palaeomagnetism of Tertiary volcanic rocks from the Ethiopian Southern Plateau and the Danakil Block, *J. Geophys.,* **40,** 203–212.

Schult, A. & Soffel, H., 1973. Palaeomagnetism of Tertiary basalts from Libya, *Geophys. J. R. astr. Soc.,* **30,** 373–380.

Tchoua, F., 1974. Contribution a l'etude geologique et petrologique de quelques volcans de la Ligne du Cameroun (Mount Manengouba et Bambouto), *PhD thesis,* University Clermont-Ferrand, France.

Temdjem, R., 1986. Le Volcanisme de la Region de Ngaoundere (Adamaoua-Cameroon): etude Vulcanologique et Petrologique, *PhD thesis,* University Clermont-Ferrand.

Thouveny, N. & Williamson, D., 1988. Paleomagnetic study of the Holocene and Upper Pleistocene sediments from lake Barombi Mbo, Cameroon: first result, *Phys. Earth planet. Int.,* **52,** 193–206.

Ubangoh, R.U., 1991. The 1991 Explosive earthquake of Mt. Cameroon, in *AK Seismic monitoring assistance 3-year project report (University of Leeds) ODA file nos. AF 87/88–89/91, 012/85/001.*

Ubangoh, R.U., 1998. Estudo paleomagnético do vulcanismo terciário da Republica dos Camarões, *PhD thesis,* São Paulo, Brazil.

Watkins, N.D., Richardson, A. & Mason, K.G., 1968. Paleomagnetism of the Macaronesian Insular region: the cape Verde Islands, *Geophys. J.R. astr. Soc.,* **16,** 119–131.

Watson, G.S., 1956. A test for randomness of directions, *Mon. Not. R. astr. Soc., Geophys. Suppl.,* **7,** 160–161.

Wilson, J.B., 1970. Permanent aspects of the Earth's non-dipole magnetic field in Upper Tertiary times, *Geophys. J.R. astr. Soc.,* **19,** 417–426.

Zijderverld, J.D.A., 1967. A.C. demagnetization of rocks: analysis results, in *Methods in Paleomagnetism,* pp. 254–286, eds Collinson, D.W., Creer, K.M. & Runcorn, S.K., Elsevier, Amsterdam.